GEOPHYSICS, VOL. 50, NO. 4 (APRIL 1985); P. 571–581, 25 FIGS., 2 TABLES.

Relationships between compressional-wave and shear-wave velocities in clastic silicate rocks

J. P. Castagna*, M. L. Batzle*, and R. L. Eastwood*

ABSTRACT

New velocity data in addition to literature data derived from sonic log, seismic, and laboratory measurements are analyzed for clastic silicate rocks. These data demonstrate simple systematic relationships between compressional and shear wave velocities. For water-saturated clastic silicate rocks, shear wave velocity is approximately linearly related to compressional wave velocity and the compressional-to-shear velocity ratio decreases with increasing compressional velocity. Laboratory data for dry sandstones indicate a nearly constant compressional-to-shear velocity ratio with rigidity approximately equal to bulk modulus. Ideal models for regular packings of spheres and cracked solids exhibit behavior similar to the observed water-saturated and dry trends. For dry rigidity equal to dry bulk modulus, Gassmann's equations predict velocities in close agreement with data from the water-saturated rock.

INTRODUCTION

The ratio of compressional to shear wave velocity (V_p/V_s) for mixtures of quartz, clays, and other rock-forming minerals is significant in reflection seismology and formation evaluation. In this paper, we investigate the V_p/V_s ratio in binary and ternary mixtures of quartz, clays, and fluids.

The classic paper by Pickett (1963) popularized the use of the ratio of compressional to shear wave velocities as a lithology indicator. Figure 1, reproduced from Pickett's paper, shows the distinct difference in V_p/V_s for limestones, dolomites, and clean sandstones. Nations (1974), Eastwood and Castagna (1983), and Wilkens et al. (1984) indicated that V_p/V_s for binary mixtures of quartz and carbonates tends to vary almost linearly between the velocity ratios of the end members with changing composition.

Figure 2 shows compressional and shear wave velocities for minerals reported in the literature (e.g., Birch, 1966; Christensen, 1982). These velocities are calculated from single crystal data and represent isotropic aggregates of grains. Also plotted is an extrapolation of Tosaya's (1982) empirical relation for V_p and V_s in shaly rocks to 100 percent clay and zero porosity. The position of this "clay point" depends upon the particular clay mineral, and it is plotted only to indicate roughly the neighborhood in which velocities of clay minerals are to be expected. Interpretation of sedimentary rock velocities should be done in the context of these mineral velocities.

We establish general V_p/V_s relationships for clastic silicate rocks by comparing in-situ and laboratory data with theoretical model data. Available velocity information is examined for data from water-saturated mudrocks and sandstones. We examine laboratory data from dry sandstone and compare with simple sphere pack and cracked media theoretical model data. Data from water-saturated rocks are similarly investigated. The results of the relationships established between V_p and V_s are then applied to calculations of rock dynamic moduli. Finally, the general V_p-V_s trends versus depth are estimated for Gulf Coast clastics.

EXPERIMENTAL TECHNIQUES

We have combined a variety of in-situ and laboratory measurements for clastic silicate rocks that includes our data and data extracted from the literature. In-situ compressional and shear wave velocities were obtained by a number of sonic and seismic methods which are described in detail in the literature cited. Due to the development of shear wave logging, it is now possible to obtain shear wave velocities routinely over a wide range of borehole/lithologic conditions with few sampling problems and in quantities which were never before available (Siegfried and Castagna, 1982).

Both our laboratory data and laboratory data we assembled from the literature were obtained using the pulse transmission technique. Compressional and shear wave velocities are determined for a sample by the transit time of ultrasonic pulses (approximately 200 kHz to 2 MHz). The jacketed sample is placed in either a pressure vessel or load frame so that stresses can be applied. Temperature and pore fluid pressure can also be controlled. Details of the techniques are found in Gregory (1977) or Simmons (1965).

Manuscript received by the Editor March 12, 1984; revised manuscript received October 12, 1984.
*ARCO Oil and Gas Company, Exploration and Production Research, P.O . Box 2819, Dallas, TX.

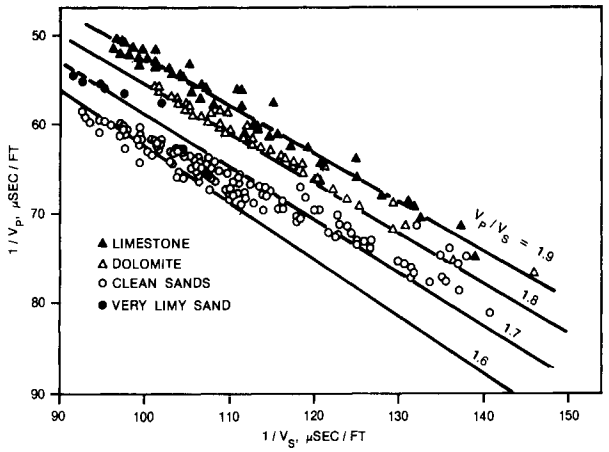

FIG. 1. Laboratory measurements on limestones, dolomites, and sandstones from Pickett (1963). V_p = compressional velocity, V_s = shear velocity.

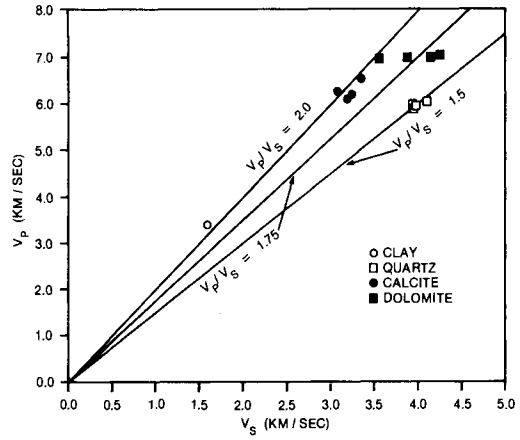

FIG. 2. Compressional and shear velocities for some minerals.

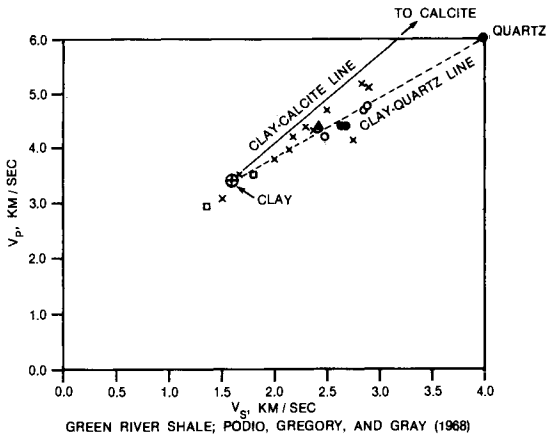

FIG. 3. Ultrasonic laboratory measurements for various mudrocks.

OBSERVATIONS IN MUDROCKS

We define mudrock as clastic silicate rock composed primarily of clay- or silt-sized particles (Blatt et al., 1972). Lithified muds are composed primarily of quartz and clay minerals. Owing to the difficulty associated with handling of most mudrocks, laboratory measurements on these rocks are not commonly found in the literature. Measurements that do exist are generally biased toward highly lithified samples.

Figure 3 is a V_p-versus-V_s plot of laboratory measurements for a variety of water-saturated mudrocks. For reference, lines are drawn from the clay-point velocities extrapolated from Tosaya's data (V_p = 3.4 km/s, V_s = 1.6 km/s) to calcite and quartz points. The data are scattered about the quartz-clay line, suggesting that V_p and V_s are principally controlled by mineralogy.

In-situ sonic and field seismic measurements in mudrocks (Figure 4) form a well-defined line given by

$$V_p = 1.16V_s + 1.36, \quad (1)$$

where the velocities are in km/s. In view of the highly variable composition and texture of mudrocks, the uniform distribution of these data is surprising. We believe this linear trend is explained in part by the location of the clay point near a line joining the quartz point with the velocity of water. We hypothesize that, as the porosity of a pure clay increases, compressional and shear velocities decrease in a nearly linear fashion as the water point is approached. Similarly, as quartz is added to pure clay, velocities increase in a nearly linear fashion as the quartz point is approached. These bounds generally agree with those inferred from the empirical relations of Tosaya (1982); the exception is for behavior at very high porosities. The net result is that quartz-clay-water ternary mixtures are spread along an

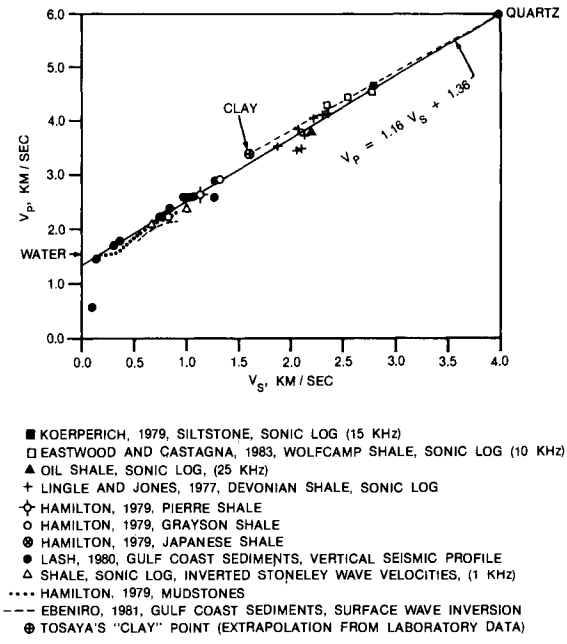

FIG. 4. Compressional and shear wave velocities for mudrocks from in-situ sonic and field seismic measurements.

elongate triangular region loosely defined by clay-water, quartz-clay, and quartz-water lines.

Figure 4 and equation (1) indicate that V_p/V_s for mudrocks is highly variable, ranging from less than 1.8 in quartz-rich rocks to over 5 in loose, water-saturated sediments. This is a direct result of the nonzero intercept at the water point.

Compressional and shear wave velocities obtained by sonic logging in geopressured argillaceous rocks of the Frio formation that exhibit clay volumes in excess of 30 percent, as determined by a neutron-density crossplot, are plotted in Figure 5. Most of the data are consistent with equation (1) and Figure 4. Figure 6 is a plot of sonic log data in shaly intervals reported by Kithas (1976). As with Figure 5, these data are well described by equation (1).

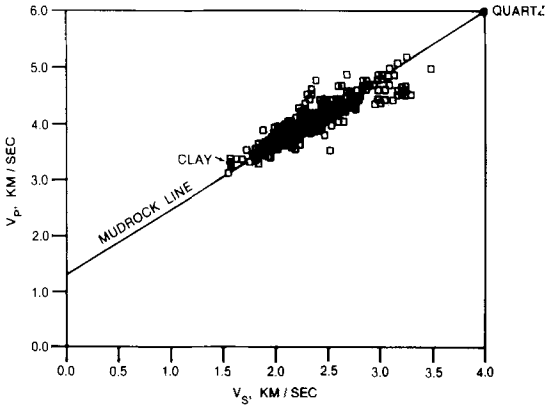

FIG. 5. Compressional and shear wave velocities for geopressured shaly rocks of the Frio formation from sonic logs.

OBSERVATIONS IN SANDSTONES

The trend of Pickett's (1963) laboratory data for clean water-saturated sandstones (Figure 7) coincides precisely with equation (1) established for mudrocks. The correspondence of V_p/V_s for sandstones and mudrocks is not entirely expected. Figure 8 is a plot of sonic log V_p and V_s data in sandstones exhibiting less than 20 percent neutron-density clay volume in the Frio formation. Except for some anomalously low V_p/V_s ratios indicative of a tight gas sandstone (verified by conventional log analysis), the data again fall along the water-saturated line established for mudrocks. Also falling along this line are sonic velocities for an orthoquartzite reported by Eastwood and Castagna (1983). In-situ measurements for shallow marine sands compiled by Hamilton (1979) fall above the line. Sonic log velocities reported by Backus et al. (1979) and Leslie and Mons (1982) in clean porous brine sands tend to fall slightly below the line (Figure 9).

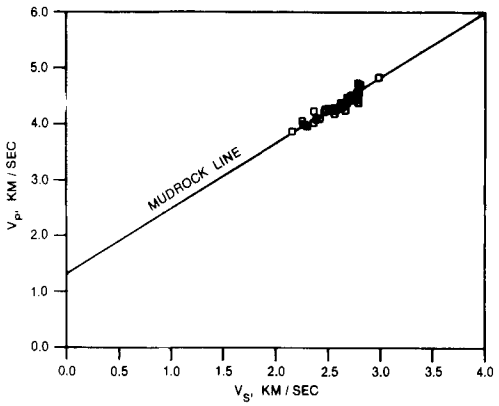

FIG. 6. Sonic data from Kithas (1976), mostly for shales.

Figure 10 is a compilation of our laboratory data for water-saturated sandstones with data from the literature (Domenico, 1976; Gregory, 1976; King, 1966; Tosaya, 1982; Johnston, 1978; Murphy, 1982; Simmons, 1965; Hamilton 1971). To first order, the data are consistent with equation (1); however, they are significantly biased toward higher V_s for a given V_p. The location of some sandstone data on the mudrock water-saturated line, although other data fall below this line, is presumably related to the sandstone texture and/or clay content.

Following the lead of Tosaya (1982), we used multiple linear regression to determine the dependence of sonic waveform-derived compressional and shear wave velocity on porosity and clay content for the Frio formation. We applied conventional log analysis to determine porosity and volume of clay (V_{cl}) from gamma ray, neutron, and density logs. The resulting relationships for the Frio formation are

$$V_p\,(\text{km/s}) = 5.81 - 9.42\phi - 2.21V_{cl} \qquad (2a)$$

and

$$V_s\,(\text{km/s}) = 3.89 - 7.07\phi - 2.04V_{cl}. \qquad (2b)$$

The correlation coefficient r for both of these relationships is .96. The equations of Tosaya (1982) for laboratory data are

$$V_p\,(\text{km/s}) = 5.8 - 8.6\phi - 2.4V_{cl}, \qquad (2c)$$

and

$$V_s\,(\text{km/s}) = 3.7 - 6.3\phi - 2.1V_{cl}. \qquad (2d)$$

The similarity between our equations and Tosaya's is evident.

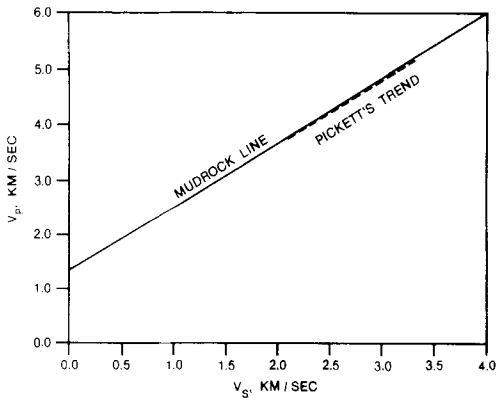

FIG. 7. Trend of sandstone compressional and shear wave velocities from Pickett (1963).

From Tosaya's equations the sonic properties of zero porosity clay are: *P*-wave transit time = 89.6 μs/ft, *S*-wave transit time = 190.5 μs/ft, and $V_p/V_s = 2.125$. The corresponding values for the Frio formation clay are: *P*-wave transit time = 84.7 μs/ft, *S*-wave transit time = 165.1 μs/ft, and $V_p/V_s = 1.95$.

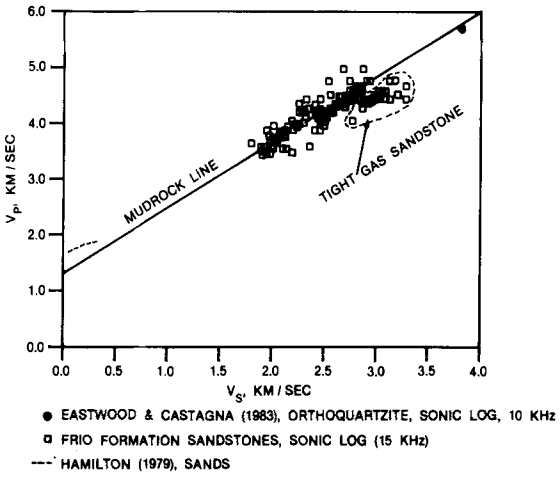

FIG. 8. Sonic log velocities in sandstones.

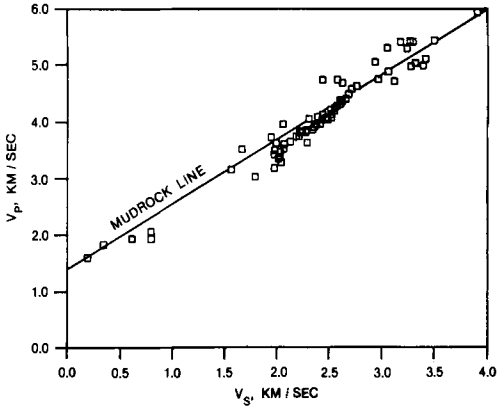

FIG. 10. Compilation of laboratory data for water-saturated sandstones, including ARCO and literature data.

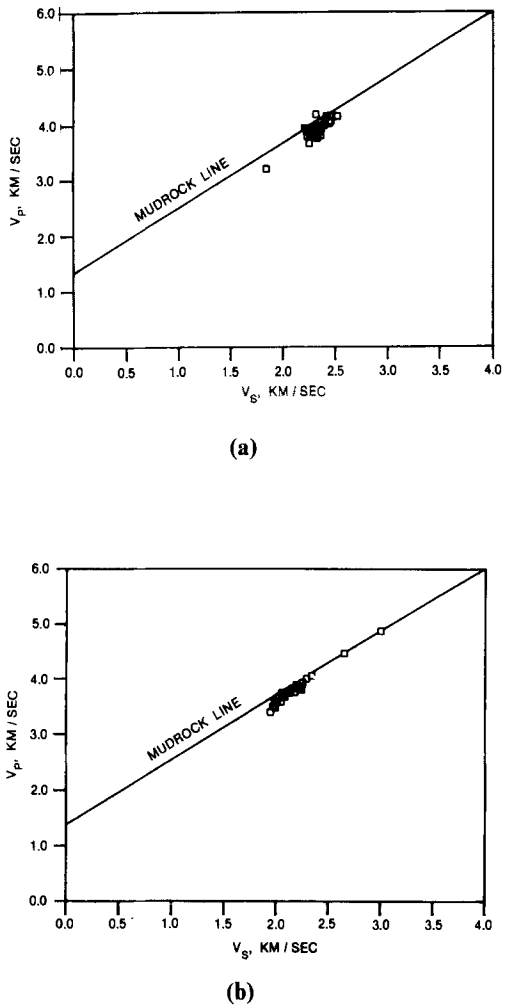

FIG. 9. Sonic log velocities for clean water-saturated sandstones. (a) Backus et al. (1979), (b) Leslie and Mons (1982).

Some algebraic manipulation yields equations which explicitly reveal the dependence of V_p/V_s on porosity and volume of clay. From equations (2a) and (2b) we get

$$V_p/V_s = 1.33 + .63/(3.89 - 7.07\phi) \tag{3a}$$

for clean sand and

$$V_p/V_s = 1.08 + 1.61/(3.89 - 2.04V_{cl}) \tag{3b}$$

for zero-porosity sand/clay mixtures. These equations reveal that increasing porosity or clay content increases V_p/V_s and that the velocity ratio is more sensitive to porosity changes.

DRY SANDSTONES: LABORATORY DATA AND IDEAL MODELS

According to Gregory (1977), Poisson's ratio is about 0.1 (corresponding to $V_p/V_s \approx 1.5$) for most dry rocks and unconsolidated sands, and it is independent of pressure. Figure 11 is a crossplot of V_p/V_s versus V_p for dry and water-saturated Berea sandstone. Note that the water-saturated points are reasonably close to the relationship defined by equation (1), whereas the dry points are nearly constant at a V_p/V_s of about 1.5. Figure 12 is a compilation of laboratory compressional and shear wave velocities for dry sandstones. The field data of White (1965) for loose sands also are included. The data fit a line having a constant V_p/V_s ratio of 1.5.

We gain some insight into the behavior of dry sandstones by considering various regular packings of spheres. The reader is referred to White (1965) and Murphy (1982) for a detailed discussion. The dry compressional (V_p^D) to shear (V_s^D) velocity ratio, as a function of Poisson's ratio (v) of solid spheres, is

$$V_p^D/V_s^D = [(2 - \nu)/(1 - \nu)]^{1/2} \tag{4a}$$

for a simple cubic packing (SC) of spheres;

$$V_p^D/V_s^D = [4(3 - \nu)/(6 - 5\nu)]^{1/2} \tag{4b}$$

for a hexagonal close packing (HCP) of spheres; and

$$V_p^D/V_s^D = \sqrt{2} \tag{4c}$$

for a face-centered cubic (FCC) packing. For HCP and FCC packings propagation directions are (1, 0, 0).

These relations are valid only at elevated confining pressures when the packings have sufficiently high bulk and shear moduli to propagate elastic waves. The velocity ratio cancels the pressure dependence: however, this pressure restriction should be kept in mind.

From equations (4a) through (4c) we see that dry V_p/V_s is constant or dependent only upon Poisson's ratio of the spheres (v). For quartz spheres ($v \approx 0.1$), dry V_p/V_s is virtually the same for these packings (FCC = 1.41, HCP = 1.43, SC = 1.45).

Dry V_p/V_s ratios based on these regular packings of spheres (Figure 13) indicate that the elastic properties of the grains are of secondary importance. The maximum range of dry V_p/V_s is for SC, and varies only from $\sqrt{2}$ to $\sqrt{3}$ when Poisson's ratio of the spheres varies from 0 to 0.5. For all practical purposes, dry V_p/V_s for packings of common rock-forming minerals is from 1.4 to 1.5.

For real rocks, of course, a number of complicating factors must be considered. One of these is the presence of microfractures or pores of low aspect ratio. One means of studying the effects of microfractures is to make velocity measurements on samples before and after cracking by heat cycling. Figure 14 shows the results of heat cycling on dry sandstones obtained by Aktan and Farouq Ali (1975). The effect of the addition of microfractures is to reduce both compressional and shear wave velocities in a direction parallel to the dry line, maintaining a nearly constant V_p/V_s.

Further insight into the effect of microfractures is provided by modeling the elastic moduli of solids with various pore aspect ratio spectra utilizing the formulation of Toksöz et al. (1976). This theory assumes randomly oriented and distributed noninteracting elliptical pores and, therefore, may not be valid for highly porous or shaly rocks.

As an example, we computed the V_p/V_s relationship for the inverted Boise sandstone pore spectrum (Cheng and Toksöz, 1976). This was done by maintaining the same relative concentrations among the aspect ratio distribution but uniformly increasing the entire distribution to increase the total porosity. Our intent was to show that aspect ratio distributions thought to be characteristic of actual rocks produce behavior in close agreement with observed trends. We do not imply that these distributions are quantitatively applicable to real rocks. Except

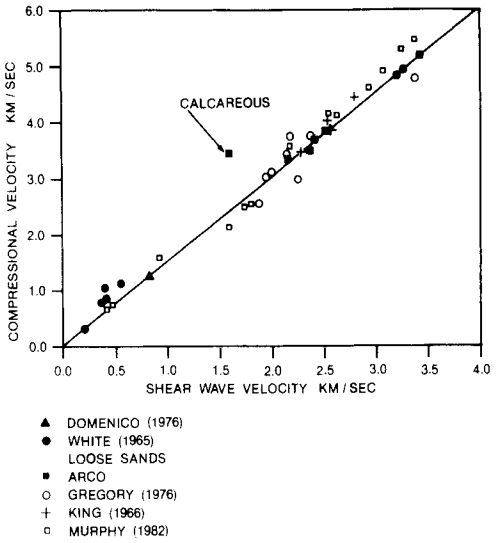

FIG. 12. Laboratory measurements for V_s and V_p for dry sandstones. Note that one sandstone with calcite cement plots well above the line.

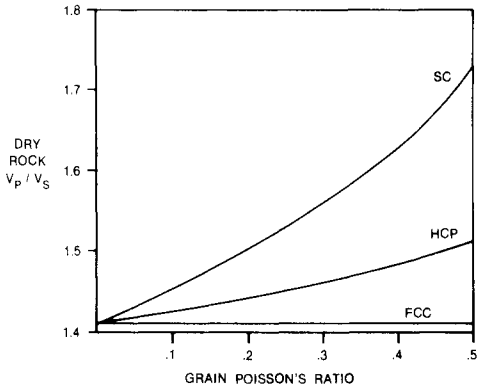

FIG. 13. Calculated V_p/V_s for regular packings of spheres versus Poisson's ratio (v) of the sphere material. SC = simple cubic packing, HCP = hexagonal close packing, FCC = face-centered cubic packing.

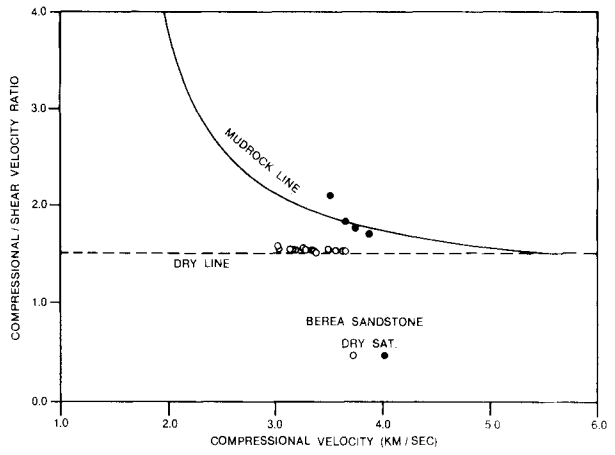

FIG. 11. Ultrasonic measurements of V_p/V_s for a dry and water-saturated Berea sandstone sample. The various points were obtained at different effective pressures.

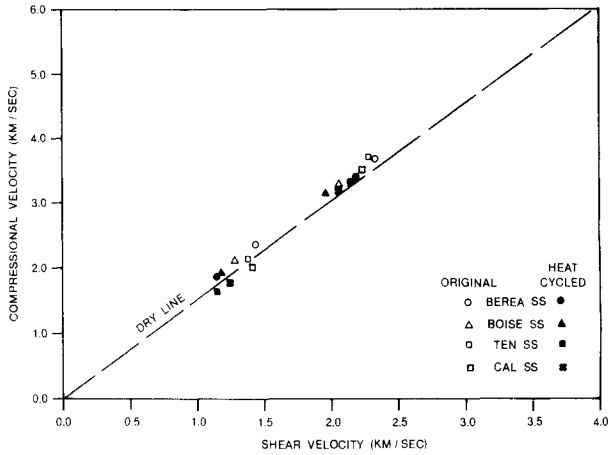

FIG. 14. The results of Aktan and Farouq Ali (1975) for several dry sandstones before and after heat cycling. Data are plotted for measurements at high and low confining pressures.

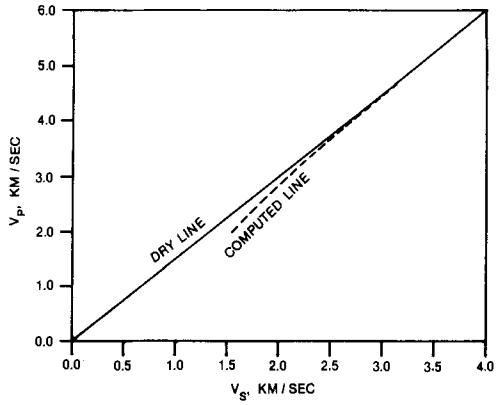

FIG. 15. Calculated V_s and V_p from the formulation of Cheng and Toksöz (1979) using the inverted pore aspect ratio spectrum of Boise sandstone.

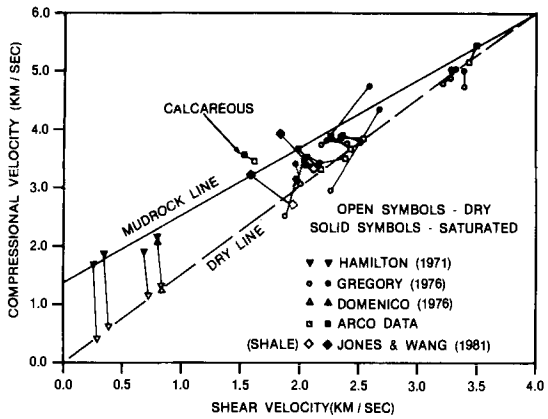

FIG. 16. Ultrasonic laboratory data for various sandstones under both dry and saturated conditions. Dry (open symbols) and saturated (solid symbols) data are plotted for the same effective pressure conditions and joined by tie lines.

for high crack concentrations (low velocities) where the limits of the model may be exceeded, the computed line for dry Boise sandstone is in excellent agreement with the observed dry sandstone line (Figure 15). It is interesting to note that an identical computed line is obtained when all cracks with pore aspect ratios less than 0.1 are closed. This is consistent with the results of Atkan and Farouq Ali (1975) shown in Figure 14. The addition of microfractures to a dry rock lowers V_p and V_s, but does not change the V_p/V_s ratio appreciably.

To summarize, we examined two extreme cases for dry rocks by two different models: (1) regular packings of spheres and (2) cracked solids. Both models predict a nearly constant V_p/V_s for dry sandstone, which is consistent with experimental observation.

SATURATED SANDSTONES: LABORATORY DATA AND IDEAL MODELS

Figure 16 shows V_p/V_s relationships for dry and water-saturated sandstones. Lines join measurements made on single dry and water-saturated samples under the same effective pressure conditions. Qualitatively, the data from water-saturated sandstones are consistent with equation (1) but tend toward higher V_s for a given V_p.

Given the compressional and shear wave velocities obtained in the laboratory for dry sandstones, we use Gassmann's (1951) equations to compute velocities when these rocks are saturated with water. Gassmann's equations are:

$$K_W = K_S \frac{K_D + Q}{K_S + Q}, \tag{5a}$$

$$Q = \frac{K_F(K_S - K_D)}{\phi(K_S - K_F)}, \tag{5b}$$

$$\mu_W = \mu_D, \tag{5c}$$

and

$$\rho_W = \phi\rho_F + (1 - \phi)\rho_S, \tag{5d}$$

where K_W is the bulk modulus of the wet rock, K_S is the bulk modulus of the grains, K_D is the bulk modulus of the dry frame, K_F is the bulk modulus of the fluid, μ_W is the shear modulus of the wet rock, μ_D is the shear modulus of the dry rock, ρ_W is the density of the wet rock, ρ_F is the density of the fluid, ρ_S is the density of the grains, and ϕ is the porosity. Figure 17 is a plot of computed (from Gassmann's equations) and measured saturated compressional and shear wave velocities. Although the individual points do not always coincide, the computed and measured data follow the same trend.

We also can apply Gassmann's equations to the equations for dry regular packing arrangements of spheres given by Murphy (1982). Figure 18 shows the relationship between V_p and V_s for water-saturated SC, HCP, and FCC packings. Note that the packings of equal density (FCC and HCP) yield virtually the same curve. The curves obtained for these simple packings are qualitatively consistent with the low-velocity experimental data of Hamilton (1971) and Domenico (1976).

For water-saturated rock, the formulation of Toksöz et al. (1976) predicts that the addition of microfractures will change the V_p-V_s relationship (Figure 19). The inverted Boise sandstone pore aspect ratio spectrum yields a line close to equation (1). Closing all cracks with aspect ratios less than 0.1 yields a line which lies below equation (1). Thus, we might expect data for clean porous sandstones dominated by equant porosity to lie slightly below the line defined by equation (1), whereas tight sandstones with high concentrations of elongate pores would tend to lie along this line. Verification of this hypothesis is left as an objective of future research.

A good description of the water-saturated V_p-V_s relationship for sandstones is provided by the following formulation. The dry line established with laboratory data ($V_p/V_s \approx 1.5$) means that dry bulk modulus (K_D) is approximately equal to dry rigidity (μ_D)

$$\mu_D \approx K_D. \tag{6}$$

These are exactly equal when

$$V_p^D/V_s^D = 1.53. \tag{7}$$

From equation (5c) it follows that

$$K_D \approx \mu_D = \mu_W. \tag{8}$$

Thus, the saturated shear velocity can be obtained from the dry bulk modulus by

$$V_s^2 \approx \frac{K_D}{\rho_W}. \tag{9}$$

The wet bulk modulus is given by

$$K_W = \rho_W(V_p^2 - \tfrac{4}{3}V_s^2). \tag{10}$$

Equations (9) and (10) and Gassmann's equations [(5a) through (5d)] allow computation of V_s given V_p, ϕ, and the grain and fluid densities and bulk moduli.

We computed shear-wave velocities for sandstone core porosities and sonic log compressional velocities given by Gregory et al. (1980) for depths from 2 500 to 14 500 ft in two wells 500 ft apart in Brazoria County, Texas. Figure 20 shows that the resulting V_p-V_s relationship is in excellent agreement with our sandstone observations.

Similarly, in Table 1 we compare the calculated shear velocities to the measured laboratory values. The differences are usually less than 5 percent, demonstrating excellent agreement with the theory. Since part of these differences must be due to experimental error and to our assumption that the matrix is 100 percent quartz, we consider the agreement remarkable. Additionally, Gassmann's equations are strictly valid only at low frequencies. Further corrections can be applied to account for dispersion. The Holt sand sample, which gives the largest discrepancy in Table 1, illustrates the importance of the assumption that dry bulk modulus is equal to dry rigidity [equation (6)]. The dry V_p/V_s for this Holt sand sample is 2.17 (Table 2), far different from the ratio of 1.53 required for equality of dry bulk and shear moduli. This variation is probably due to the high carbonate cement component of this rock. However, given this measured dry ratio, we can still apply Gassmann's equations to calculate the water-saturated values. As shown in Table 2, these predicted values are virtually identical to the measured velocities.

For clean sandstones at high pressures and with moderate porosities, porosity is often estimated by the empirical time-average formula (Wyllie et al., 1956),

$$\phi \simeq \frac{1/V_p - 1/V_p^s}{1/V_p^f - 1/V_p^s}, \tag{11}$$

where V_p^s is the grain compressional velocity and V_p^f is the fluid velocity. Figure 21 shows the V_p-V_s relationship predicted by

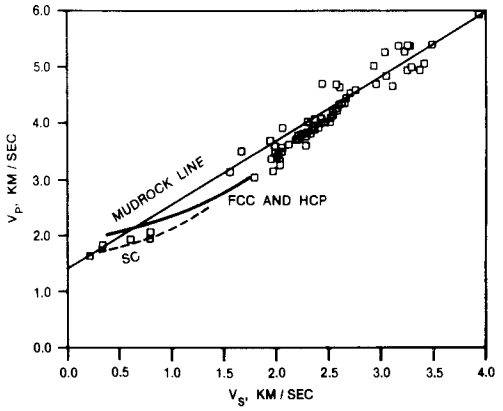

FIG. 18. Calculated V_s and V_p for saturated regular packings of quartz spheres using the calculated dry velocities and Gassmann's equations.

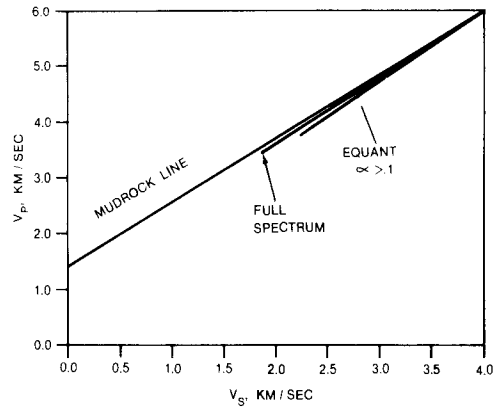

FIG. 19. Calculated V_s and V_p for Boise sandstone based on the formulation of Cheng and Toksöz (1979).

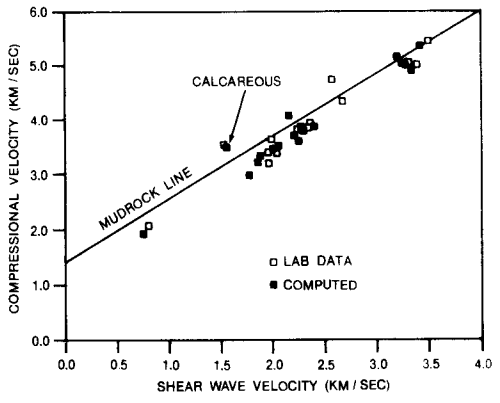

FIG. 17. Measured (open symbols) versus computed (solid symbols) V_s and V_p using the dry data from Figure 12 and Gassmann's equations.

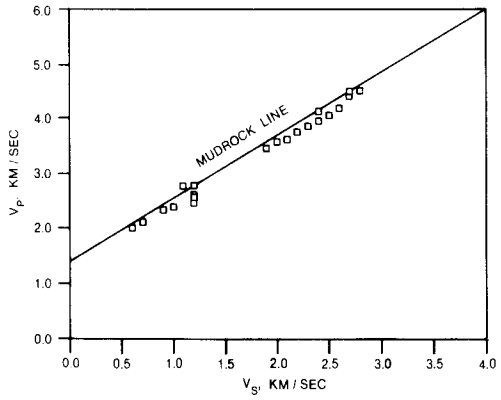

FIG. 20. Comparison of measured V_p with calculated V_s for sandstones from two wells as reported by Gregory et al. (1980). Calculations are based on measured wet V_p and porosity using Gassmann's equations and dry bulk modulus equal to dry rigidity.

Table 1. Holt sand: Comparison of observed water-saturated shear velocities with those calculated using the measured water-saturated compressional velocities and porosities. The calculations were based on Gassmann's equations and the assumption that $K_D \simeq \mu_D$.

Rock	Reference	V_p	Porosity	Predicted V_s	Observed V_s	Percent Error
Berea	Johnston (1978)	3.888	18.4	2.330	2.302	1.2
Berea	Johnston (1978)	4.335	18.4	2.700	2.590	4.2
Navajo	Johnston (1978)	4.141	16.4	2.520	2.430	3.7
Navajo	Johnston (1978)	4.584	16.4	2.890	2.710	6.6
Gulf Coast sand	Gregory (1976)	3.927	21.7	2.380	2.367	0.5
Gulf Coast sand	Gregory (1976)	3.185	21.7	1.730	1.975	−12.4
Boise	Gregory (1976)	3.402	26.8	1.970	1.960	.5
Boise	Gregory (1976)	3.533	26.8	2.080	2.073	.3
Travis peak	Gregory (1976)	4.732	4.45	2.860	2.581	10.8
Travis peak	Gregory (1976)	4.990	4.45	3.110	3.284	−5.3
Travis peak	Gregory (1976)	4.342	8.02	2.590	2.667	−2.9
Travis peak	Gregory (1976)	5.001	8.02	3.180	3.391	−6.2
Bandera	Gregory (1976)	3.492	17.9	1.970	2.032	−3.1
Bandera	Gregory (1976)	3.809	17.9	2.250	2.240	.4
Ottawa	Domenico (1976)	2.072	37.74	.740	.801	−7.6
Sample no. MAR	ARCO data	5.029	1.0	3.200	3.315	−3.5
Sample no. MAR	ARCO data	5.438	1.0	3.420	3.496	−2.2
Sample no. MDP	ARCO data	3.377	21.0	1.900	2.047	−7.2
Sample no. MDP	ARCO data	3.862	21.0	2.320	2.350	−1.3
Berea	ARCO data	3.642	19.0	2.120	1.992	6.4
Berea	ARCO data	3.864	19.0	2.310	2.267	4.3
Berea	ARCO data	3.510	19.0	2.000	1.680	19.0
Berea	ARCO data	3.740	19.0	2.200	2.130	3.8
St. Peter	Tosaya (1982)	5.100	6.6	3.250	3.420	−5.0
St. Peter	Tosaya (1982)	4.880	7.2	3.060	3.060	0.0
St. Peter	Tosaya (1982)	4.500	4.2	2.610	2.680	−2.6
St. Peter	Tosaya (1982)	4.400	7.5	2.630	2.600	1.2
St. Peter	Tosaya (1982)	4.400	5.0	2.540	2.600	−2.3
St. Peter	Tosaya (1982)	3.950	18.8	2.380	2.420	−1.6
St. Peter	Tosaya (1982)	3.600	19.6	2.090	2.070	1.0
St. Peter	Tosaya (1982)	3.170	14.5	1.580	1.560	1.3
Holt sand	ARCO data	3.546	16.3	1.990	1.539	29.3

Table 2. Water-saturated sandstones: A recalculation of velocities for the Holt Sand (Table 1) for which $K_D \neq \mu_D$. New water-saturated values are computed using both the V_p and V_s measured for the dry rock.

Holt Sand	
Porosity	16.3%
Water-saturated V_p (laboratory)	3.546 km/s
Water-saturated V_s (laboratory)	1.539 km/s
Water-saturated V_s (predicted from porosity and water-saturated V_p)	1.990 km/s
Percent error	29.3%
Dry V_p (laboratory)	3.466 km/s
Dry V_s (laboratory)	1.599 km/s
Dry V_p/V_s (laboratory)	2.17 km/s
Water-saturated V_p (predicted from dry data)	3.519 km/s
Percent error	−.8%
Water-saturated V_s (predicted from dry data)	1.540 km/s
Percent error	.1%

equations (5), (9), (10), and (11). This "time-average" line describes the laboratory data from water-saturated conditions presented in Figure 10 extremely well. Recalling the results of crack modeling shown in Figure 19, one explanation for the validity of this empirical formula would be the dominance of pores of high aspect ratio.

DISCUSSION OF RESULTS: DYNAMIC ELASTIC MODULI RELATIONSHIPS

Compressional and shear velocities, along with the density, provide sufficient information to determine the elastic parameters of isotropic media (Simmons and Brace, 1965). These parameters proved useful in estimating the physical properties of soils and characteristics of formations (see, for example, Richart, 1977). However, the relationships given by equation (1) for mudrocks or Gassmann's equations and equation (6) for sandstones fix V_s in terms of V_p. Hence, the elastic parameters can be determined for clastic silicate rocks from conventional sonic and density logs. This explains in part why Stein (1976) was successful in empirically determining the properties of sands from conventional logs.

In this discussion we assumed that equation (1) holds to first order for all clastic silicate rocks, with the understanding that Gassmann's equations might be used to obtain more precise results in clean porous sandstones if necessary. For many rocks, particularly those with high clay content, the addition of water softens the frame, thereby reducing the bulk elastic moduli. The following empirical relationships are, therefore, not entirely general but are useful for describing the wide variety of data presented here. As shown in Figure 22, bulk and shear moduli are about equal for dry sandstones. Adding water causes the bulk modulus to increase. This effect is most pronounced at

higher porosities (lower moduli). Water-saturated bulk modulus normalized by density is linearly related to compressional velocity (Figure 23):

$$\frac{K_W}{\rho_W} \approx 2bV_p^W - b^2, \qquad b = 1.36 \text{ km/s}. \tag{12}$$

Water-saturated rigidity normalized by density is nonlinearly related to wet compressional velocity:

$$\frac{\mu_W}{\rho_W} \approx \frac{3}{4}(V_p^W - b)^2. \tag{13}$$

Dry bulk modulus and rigidity normalized by density are given by

$$\frac{\mu_D}{\rho_D} \approx \frac{K_D}{\rho_D} \approx \frac{3}{7}(V_p^D)^2. \tag{14}$$

Poisson's ratio for water-saturated rock is approximately linearly related to compressional velocity (Figure 24). Poisson's ratio of air-saturated rock is constant.

DISCUSSION OF RESULTS: SEISMOLOGY AND FORMATION EVALUATION

In recent years there has been increased use of V_p, V_s, and V_p/V_s in seismic exploration for estimation of porosity, lithology, and saturating fluids in particular statigraphic intervals. The above analysis both complicates and enlightens such interpretation. It is clear that clay content increases the ratio V_p/V_s, as does porosity. The analyses of Tosaya (1982) and Eastwood and Castagna (1983) and equations (3a) and (3b) indicate that V_p/V_s is less sensitive to variation of clay content than to variation of porosity. However, the range of variation in clay content may be larger. Thus, V_p/V_s can be grossly dependent upon clay content.

Figure 25 shows V_p/V_s computed as a function of depth in the Gulf Coast for noncalcareous shales and clean porous sandstones that are water-saturated. The compressional velocity and porosity data given in Gregory (1977) are used to establish the variation with depth. Equation (1) is used to predict V_s for shales, and Gassmann's equations are used for sandstones. At a given depth, shale velocity ratios are on the order of 10 percent higher than sandstone velocity ratios.

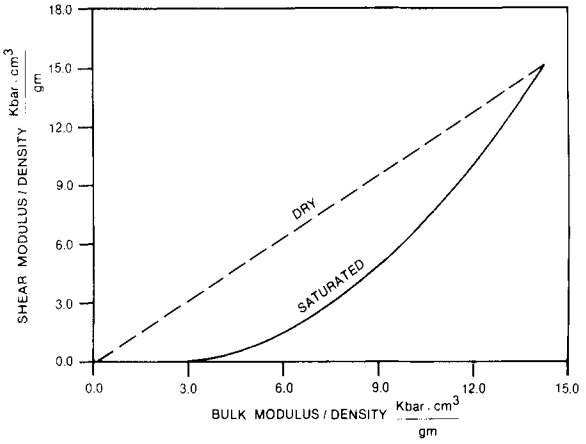

FIG. 22. The computed relationships between the bulk and shear moduli (normalized by density) based on the observed V_s and V_p trends.

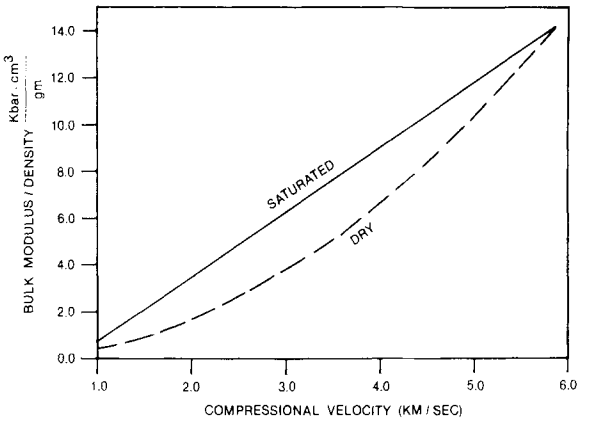

FIG. 23. The computed relationships between the bulk modulus (normalized by density) and V_p based on the observed V_s and V_p trends.

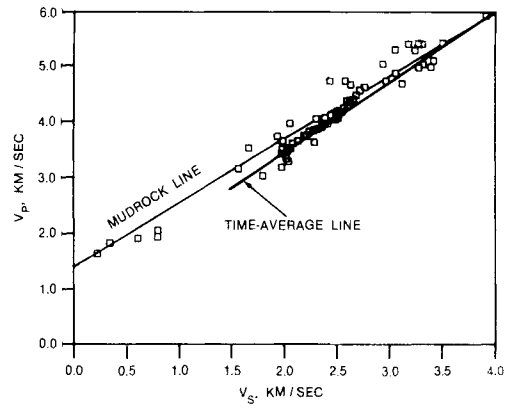

FIG. 21. Calculated V_s and V_p based on the time-average equation and Gassmann's equations.

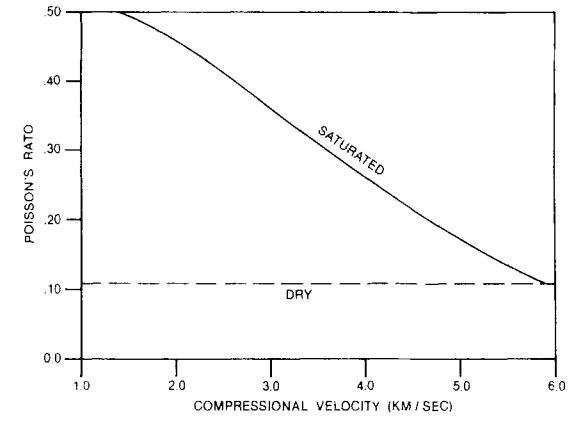

FIG. 24. The computed relationships between Poisson's ratio and V_p based on the observed V_s and V_p trends.

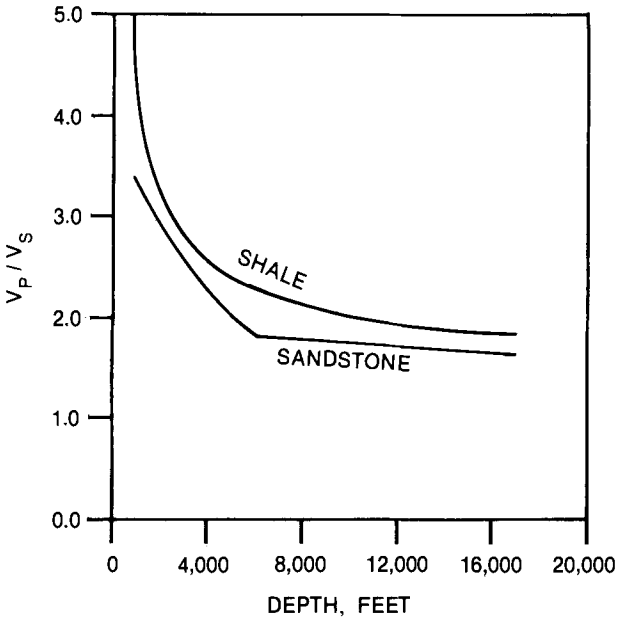

FIG. 25. V_p/V_s computed as a function of depth for selected Gulf Coast shales and water-saturated sands.

These conclusions are somewhat at odds with conventional wisdom that V_p/V_s equals 1.5 to 1.7 in sandstones and is greater than 2 in shales. Clearly, mapping net sand from V_p/V_s is not as straightforward as conventional wisdom would imply.

In clastic silicates, shear wave velocities for elastic moduli estimation or seismic velocity control may be estimated from equation (1) and/or Gassmann's equations and conventional logs. Alternatively, our relationships indicate that when V_p and V_s are used together, they can be sensitive indicators of both gas saturation and nonclastic components in the rock. Gas saturation will move the V_p/V_s toward the dry line in Figure 16. Nonclastic components can also move the ratio off the mudrock line, as shown by the Holt sand sample marked as calcareous in Figure 16.

The possibly ambiguous interpretation of lithology and porosity from V_p, V_s, and V_p/V_s in seismic exploration also applies to log analysis. However, because sonic logs are generally a part of usual logging programs, the interpretation of full waveform sonic logs should be made in the context of other logging information (as we did) to obtain equations (2a) and (2b). Other logs which are sensitive to clay content and porosity (e.g., neutron and gamma-ray) are needed to evaluate the details of how porosity and clay content separately affect clastic rocks. In gas-bearing and highly porous zones where the time-average equation fails, combined V_p and V_s information may potentially be used in porosity determination.

Assuming that the time-average equation works for compressional transit times and that dry incompressibility equals dry rigidity, Gassmann's equations yield a nearly linear relationship between shear wave transit time and porosity. This relationship is well described by a time-average equation

$$\phi = \frac{1/V_s - 1/V_s^s}{1.12 \text{ s/km} - 1/V_s^s} \qquad (15)$$

where V_s^s is the grain shear wave velocity. The constant 1.12 s/km is used in place of fluid transit time. This equation should be superior to the compressional wave time-average equation for porosity estimation when there is significant residual gas saturation in the flushed zone.

SUMMARY AND CONCLUSIONS

To first order, we conclude that shear wave velocity is nearly linearly related to compressional wave velocity for both water-saturated and dry clastic silicate sedimentary rocks. For a given V_p, mudrocks tend toward slightly higher V_p/V_s than do clean porous sandstones.

For dry sandstones, V_p/V_s is nearly constant. For wet sandstones and mudstones, V_p/V_s decreases with increasing V_p. Water-saturated sandstone shear wave velocities are consistent with those obtained from Gassmann's equations. The water-saturated linear V_p-versus-V_s trend begins at V_p slightly less than water velocity and $V_s = 0$, and it terminates at the compressional and shear wave velocities of quartz. The dry sandstone linear V_p-versus-V_s trend begins at zero velocity and terminates at quartz velocity. Dry rigidity and bulk modulus are about equal.

Theoretical models based on regular packing arrangements of spheres and on cracked solids yield V_p-versus-V_s trends consistent with observed dry and wet trends.

We believe that the observed V_p-versus-V_s-relationship for wet clastic silicate rocks results from the coincidental location of the quartz and clay points. The simple sphere-pack models indicate that the low-velocity, high-porosity trends are largely independent of the mineral elastic properties. As the porosity approaches zero, however, the velocities must necessarily approach the values for the pure mineral. In this case, clay and quartz fall on the extrapolated low-velocity trend.

REFERENCES

Aktan, T., and Farouq Ali, C. M., 1975, Effect of cyclic and in situ heating on the absolute permeabilities, elastic constants, and electrical resistivities of rocks: Soc. Petr. Eng., 5633.

Backus, M. M., Castagna, J. P., and Gregory, A. R., 1979, Sonic log waveforms from geothermal well, Brazoria Co., Texas: Presented at 49th Annual International SEG Meeting, New Orleans.

Birch, F., 1966, Compressibility; elastic constants, *in* Handbook of physical constants, Clark, S. P., Jr., Ed., Geol. Soc. Am., Memoir 97, 97–174.

Blatt, H., Middleton, G. V., and Murray, R. C., 1972, Origin of sedimentary rocks: Prentice-Hall, Inc.

Cheng, C. H., and Toksöz, M. N., 1976, Inversion of seismic velocities for the pore aspect ratio spectrum of a rock: J. Geophys. Res., **84**, 7533–7543.

Christensen, N. J., 1982, Seismic velocities, *in* Carmichael, R. S., Ed., Handbook of physical properties of rocks, **II**: 2-227, CRC Press, Inc.

Domenico, S. N., 1976, Effect of brine-gas mixture on velocity in an unconsolidated sand reservoir: Geophysics, **41**, 887–894.

Eastwood, R. L., and Castagna, J. P., 1983, Basis for interpretation of V_p/V_s ratios in complex lithologies: Soc. Prof. Well Log Analysts 24th Annual Logging Symp.

Ebeniro, J., Wilson, C. R., and Dorman, J., 1983, Propagation of dispersed compressional and Rayleigh waves on the Texas coastal plain: Geophysics, **48**, 27–35.

Gassmann, F., 1951, Elastic waves through a packing of spheres: Geophysics, **16**, 673–685.

Gregory, A. R., 1977, Fluid saturation effects on dynamic elastic properties of sedimentary rocks: Geophysics, **41**, 895–921.

——— 1977, Aspects of rock physics from laboratory and log data that are important to seismic interpretation, *in* Seismic stratigraphy—application to hydrocarbon exploration: Am. Assn. Petr. Geol., Memoir 26.

Gregory, A. R., Kendall, K. K., and Lawal, S. S., 1980, Study effects of geopressured-geothermal subsurface environment of elastic properties of Texas Gulf Coast sandstones and shales using well logs, core data, and velocity surveys: Bureau of Econ. Geol. Rep., Univ. Texas, Austin.

Hamilton, E. L., 1971, Elastic properties of marine sediments: J. Geophys. Res., **76**, 579–604.

——— 1979, V_p/V_s and Poisson's ratios in marine sediments and rocks: J. Acoust. Soc. Am., **66**, 1093–1101.

Johnston, D. H., 1978, The attenuation of seismic waves in dry and saturated rocks: PhD. thesis, Mass. Inst. of Tech.

Jones, L. E. A., and Wang, H. F., 1981, Ultrasonic velocities in Cretaceous shales from the Williston Basin: Geophysics, **46**, 288–297.

King, M. S., 1966, Wave velocities in rocks as a function of changes of overburden pressure and pore fluid saturants: Geophysics, **31**, 50–73.

Kithas, B. A., 1976, Lithology, gas detection, and rock properties from acoustic logging systems: Trans., Soc. Prof. Well Log Analysts 17th Annual Logging Symp.

Koerperich, E. A., 1979, Shear wave velocities determined from long- and short-spaced borehole acoustic devices: Soc. Petr. Eng., 8237.

Lash, C. E., 1980, Shear waves, multiple reflections, and converted waves found by a deep vertical wave test (vertical seismic profiling): Geophysics, **45**, 1373–1411.

Leslie, H. D. and Mons, F., 1982, Sonic waveform analysis: applications: Trans., Soc. Prof. Well Log Analysts 23rd Annual Logging Symp.

Lingle, R., and Jones, A. H., 1977, Comparison of log and laboratory measured *P*-wave and *S*-wave velocities: Trans., Soc. Prof. Well Log Analysysts 18th Annual Logging Symp.

Murphy, W. F., III, 1982, Effects of microstructure and pore fluids on acoustic properties of granular sedimentary materials: PhD. thesis, Stanford Univ.

Nations, J. F., 1974, Lithology and porosity from acoustics and *P*-wave transit times: Log Analyst, November–December.

Pickett, G. R., 1963, Acoustic character logs and their applications in formation evaluation: J. Petr. Tech., **15**, 650–667.

Richart, F. E., Jr., 1977, Field and laboratory measurements of dynamic soil properties: Proc. DMSR 77, Karlsruhe, **1**, Prange, B., Ed., *in* Dynamical methods in soil and rock mechanics, 3–36.

Siegfried, R. W., and Castagna, J. P., 1982, Full waveform sonic logging techniques: Trans., Soc. Prof. Well Log Analysts 23rd Annual Logging Symp.

Simmons, G., 1965, Ultrasonics in geology: Proc. Inst. Electr. and Electron. Eng., **53**, 1337–1345.

Simmons, G., and Brace, W. F., 1965, Comparison of static and dynamic measurements of compressibility of rocks: J. Geophys. Res., **70**, 5649–5656.

Stein, N., 1976, Mechanical properties of friable sands from conventional log data: J. Petr. Tech., **28**, 757–763.

Toksöz, M. N., Cheng, C. H., and Timur, A., 1976, Velocities of seismic waves in porous rocks: Geophysics, **41**, 621–645.

Tosaya, C. A., 1982, Acoustical properties of clay-bearing rocks: PhD. thesis, Stanford Univ.

White, J. E., 1965, Seismic waves: Radiation, transmission and attenuation: McGraw-Hill Book Co.

Wilkens, R., Simmons, G., and Caruso, L., 1984, The ratio V_p/V_s as a discriminant of composition for siliceous limestones: Geophysics, **49**, 1850–1860.

Wyllie, M. R. J., Gregory, A. R., and Gardner, L. W., 1956, Elastic wave velocities in heterogeneous and porous media: Geophysics, **21**, 41–70.